



This open access document is posted as a preprint in the Beilstein Archives at <https://doi.org/10.3762/bxiv.2025.2.v1> and is considered to be an early communication for feedback before peer review. Before citing this document, please check if a final, peer-reviewed version has been published.

This document is not formatted, has not undergone copyediting or typesetting, and may contain errors, unsubstantiated scientific claims or preliminary data.

Preprint Title Systematic Pore Hydrophobization to Enhance the Efficiency of an Amine-Based MOF Catalyst

Authors Pricilla Matseketsa and Tendai Gadzikwa

Publication Date 16 Jan. 2025

Article Type Letter

Supporting Information File 1 Matseketsa et al-SI.pdf; 680.6 KB

ORCID® IDs Pricilla Matseketsa - <https://orcid.org/0000-0002-5000-1103>; Tendai Gadzikwa - <https://orcid.org/0000-0002-0144-467X>



License and Terms: This document is copyright 2025 the Author(s); licensee Beilstein-Institut.

This is an open access work under the terms of the Creative Commons Attribution License (<https://creativecommons.org/licenses/by/4.0>). Please note that the reuse, redistribution and reproduction in particular requires that the author(s) and source are credited and that individual graphics may be subject to special legal provisions.

The license is subject to the Beilstein Archives terms and conditions: <https://www.beilstein-archives.org/xiv/terms>.

The definitive version of this work can be found at <https://doi.org/10.3762/bxiv.2025.2.v1>

Systematic Pore Hydrophobization to Enhance the Efficiency of an Amine-Based MOF Catalyst

Pricilla Matseketsa and Tendai Gadzikwa*

Address: ¹Department of Chemistry, Kansas State University, Manhattan, Kansas 66506, United States.

Email: Tendai Gadzikwa – gadzikwa@ksu.edu

* Corresponding author

Abstract

We systematically hydrophobized an amine-based metal-organic framework (MOF) catalyst and applied the functionalized MOFs to the Knoevenagel condensation reaction. A well-defined MOF material composed of both amine- and hydroxyl-bearing linkers was reacted with a series of aliphatic isocyanates (isopropyl, *tert*-butyl, *n*-hexyl, and tetradecyl) and, incongruously, was found to preferentially react at the hydroxyl groups. This selective functionalization yielded MOFs in which the catalytically active amines are confined within highly hydrophobic pores, reminiscent of many enzyme active sites. We determined that systematically increasing the hydrophobicity of the pores results in a commensurate increase of catalyst efficiency.

Keywords

metal-organic frameworks; post-synthesis modification; supramolecular catalysis

Introduction

Most enzymatic reactions take place in multifunctional cavities in which multiple amino acid residues work cooperatively to orient and activate reactants.[1–3] These residues may also enhance covalent and/or acid-base catalysis via any combination of non-covalent interactions (hydrogen bonding, π - π stacking, hydrophobic interactions, etc)[4–6]. Inspired by enzymes, Nature's most efficient catalysts, chemists have long endeavored to synthesize catalytic materials in which multiple functional groups are isolated together in confined space.[7–9] In the solid-state, the generation of such multifunctional cavities has been pursued upon nanoporous scaffolds that include polymers of intrinsic microporosity (PIMs),[10–13] mesoporous silica materials (MSMs),[14–17] and metal-organic-frameworks (MOFs), among others. [18–20] Within this group of porous materials, MOFs boast the advantages of their crystallinity, the uniformity of their pores that are typically in the microporous range (5–20 Å), and the ability to fine-tune their pore chemical environment.[21,22] These attributes allow us to construct MOF-based catalysts with active sites that are isolated within cavities of the same size range as small molecules and whose walls are decorated with precisely located functional groups. We can rationally elaborate these functional groups to modulate catalytic performance and/or systematically investigate the influence of a particular chemical or structural property on catalyst efficiency.[23]

For examples of tailoring the pore environment in MOF-based catalysts to modulate catalytic performance, we can refer to the elegant work of Telfer and co-workers. In two separate reports, they synthesized well-defined MOFs composed of three different linkers: a proline-functionalized linker acted as the catalytic unit, while two auxiliary linkers were varied to alter catalyst activity and enantioselectivity,[24] or product-selectivity.[25] In those works, the researchers tailored their catalyst via *de novo*

solvothermal synthesis of their MOFs using differently-substituted auxiliary linkers; a non-trivial effort which involves the synthesis of several new organic linkers and their subsequent assembly into completely new frameworks (**Figure 1A**). In this report we describe how a similar tailoring of a MOF's pore environment, with consequent activity modulation, can be realized more efficiently using covalent post-synthetic modification (PSM) strategies.[26,27] Starting with a single MOF material that has both catalytic linkers and auxiliary linkers that bear reactive "tags", we can graft additional functionalities onto the auxiliaries to adjust the steric and electronic environment of the catalytic units (**Figure 1B**).

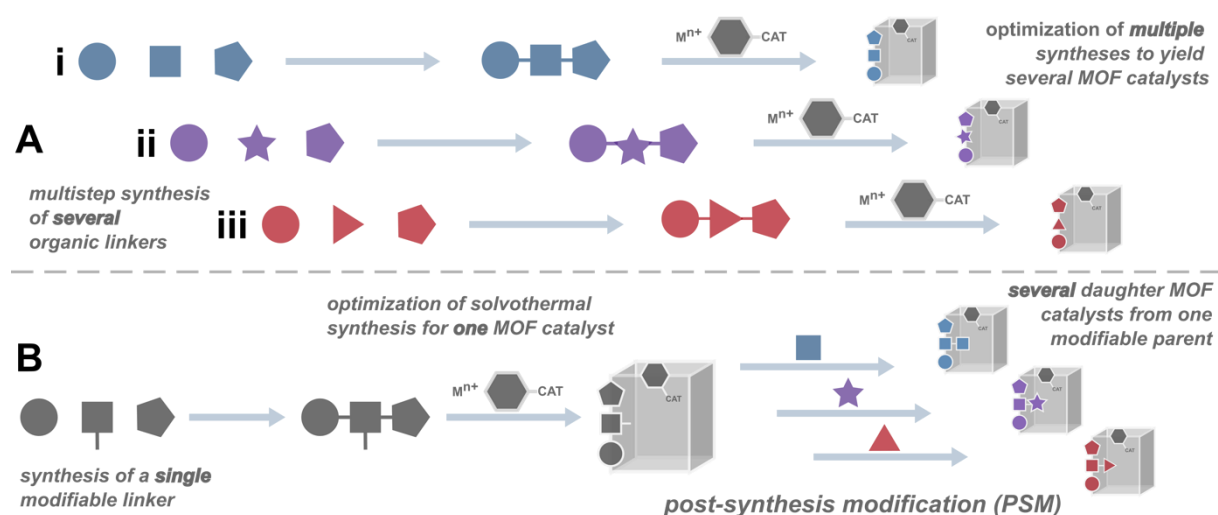


Figure 1: Schematic representation of the modulation of MOF pore environments. A: De novo synthesis of several MOFs requiring the multistep synthesis of different organic linkers. B: Synthesis of several frameworks from a single parent MOF using post-synthesis modification (PSM).

The advantages of PSM as a strategy for generating MOF-based catalysts are that we can efficiently generate several MOF catalysts from a single parent framework. Additionally, we can introduce new functionality into a MOF without changing the framework topology, thus minimizing the number of variables to consider as we study the influence of a particular property on catalytic performance. Perhaps more importantly for enzyme-inspired materials, PSM allows us to incorporate functionalities that are pertinent to catalysis but that would normally interfere with MOF assembly,

e.g. hydrogen bonding groups like –OH and –COOH that are difficult to obtain as free uncoordinated moieties within MOF pores.[28,29] Given these benefits, it is no surprise that PSM is a prevalent method for synthesizing MOF-based catalysts.[30]

On this topic, our current work was inspired by Canivet et al. who previously reported the hydrophobization of a MOF by grafting long alkyl chains to the *external* surfaces of its crystals. The active sites are believed to be coordinatively unsaturated zincs at the MOF surfaces, and their hydrophobization resulted in a greater than ten-fold increase in the initial rate of the reaction.[31] The promotion of this reaction was attributed to the repulsion of the water byproduct by the hydrophobic surface, thereby preventing its interference with the Lewis acidic catalyst surface sites, but we wondered if similar reaction acceleration of a condensation reaction could be achieved by the hydrophobization of the *internal* surfaces of an amine-based MOF catalyst.

The majority of studies of hydrophobic MOFs applied to catalysis have focused on hydrophobization to prevent catalyst deactivation due to water interference, with only a few investigating how hydrophobic pores surfaces can increase catalyst efficiency,[32,33] despite enzymes employing such a strategy. The hydrophobicity of enzyme active sites tends to improve reaction rates by increasing the binding affinity for the hydrophobic reactants and by decreasing the energy required to desolvate acid/base amino acid catalysts.[34,35] Thus, in this work, we investigate the influence of pore hydrophobicity on the amine-catalyzed Knoevenagel condensation.

The Knoevenagel condensation reaction is a vital organic reaction involving the condensation of carbonyl compounds, such as aldehydes or ketones, with active methylene compounds.[36] The resulting α,β -unsaturated carbonyl products can then be further elaborated to form natural products, therapeutic agents, polymers, pesticides and insecticides,[37] which have important applications in the pharmaceutical and agrochemical industries.[37,38] Various types of catalysts are

used to enhance the efficiency and selectivity of the Knoevenagel reaction, including Lewis acids, ureas/ thioureas, amino acids, and bases such as alkali metal hydroxides, alkali metal alkoxide, amines, etc.[36,39–42] We opted for amine-based catalysis using our modifiable framework **KSU-1**, a pillared paddlewheel MOF assembled using zinc, 2-aminobenzene-1,4-dicarboxylic acid (BDC-NH₂), and *meso*- α,β -di(4-pyridyl) glycol (DPG), as our parent MOF (**Figure 2A**). As this is a well-defined mixed-linker MOF with molecular formula $Zn_2(BDC-NH_2)_2(DPG)$, each unit cell has a 2:1 ratio of dicarboxylate to dipyridyl, and therefore in a 1:1 ratio of amine (–NH₂) to hydroxyl (–OH) groups. The Zn atoms in the paddlewheel metal clusters are coordinatively saturated,[43] thus we anticipated that only the amine group would function as the catalytic unit for the Knoevenagel reaction, while the hydroxyl group would serve as a handle through which we would tune the hydrophobicity of the catalyst.

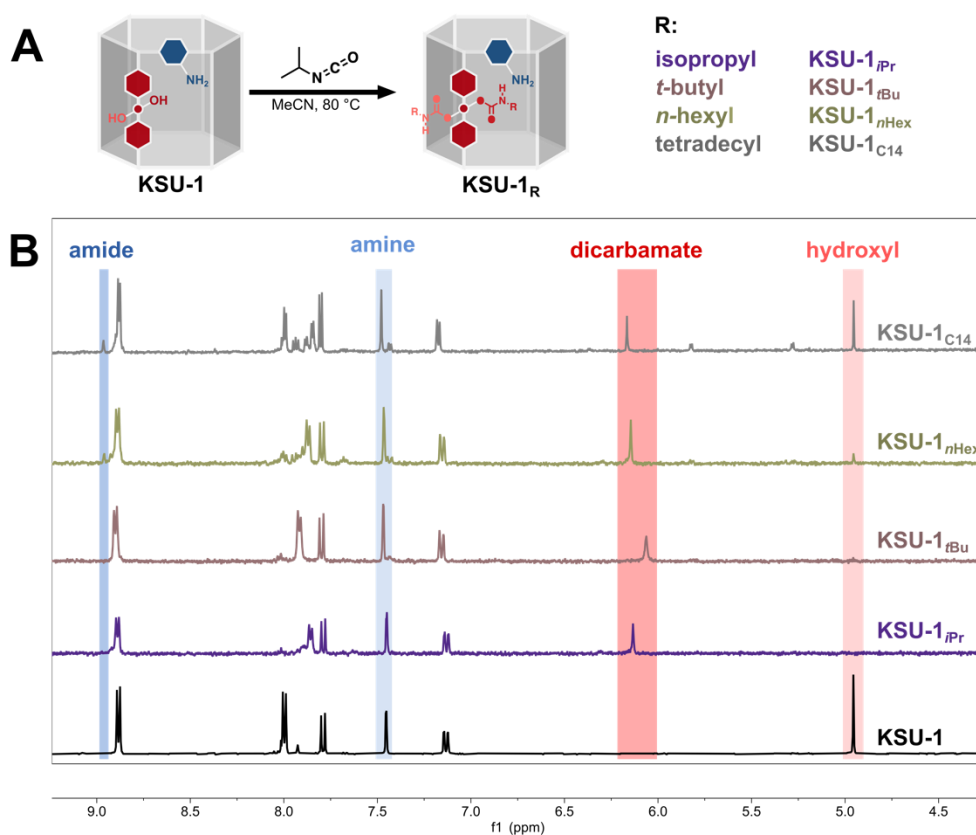


Figure 2: (A) Schematic representation of the selective reaction of **KSU-1** with aliphatic isocyanates. (B) The corresponding ¹H-NMRs of the MOF reaction products digested in a solution of D₂SO₄ in DMSO-*d*₆.

Recently, we found that isopropyl isocyanate reacts preferentially at the DPG hydroxyls of **KSU-1**;^[44] this, despite an earlier demonstration of the superior nucleophilicity of BDC-NH₂.^[45] Interestingly, this apparent reversal in reactivity was most significant with aliphatic isocyanates, while the reactivity reverted to what is expected with the use of more activated isocyanates. Subsequently, we determined that, when incubated with secondary or tertiary isocyanates, **KSU-1** reacts exclusively at the hydroxyls of the DPG linker before proceeding to react at the amines of BDC-NH₂ (**Table 1**; Entries 1-2). Thus, we had a method to generate, from a single framework, a series of amine-based MOFs whose pores are uniformly decorated with different hydrophobic groups (**Figure 2A**). Using this strategy, we quantitatively functionalized the –OH groups of **KSU-1** with isopropyl and *tert*-butyl isocyanate. While primary isocyanates were less selective, starting to react at the amines before the hydroxyl reaction was complete, we reacted **KSU-1** with *n*-hexyl and tetradecyl isocyanate as well (**Table 1**; Entries 3-4) because we wanted to use longer alkyl chains to further increase the hydrophobicity.

Table 1: Conversion of –OH and –NH₂ in the isocyanate reactions of **KSU-1**.^a

Entry	Isocyanate	–OH % conv. (stdev)	–NH ₂ % conv. (stdev)
1	Isopropyl ^b	100 (0)	0
2	<i>Tert</i> -butyl ^c	94 (5)	0
3	<i>n</i> -Hexyl ^d	73 (2)	11 (3)
4	Tetradecyl ^d	64 (5)	8 (3)

^a0.2 M in acetonitrile, 80 °C; ^b3 h; ^c4 h; ^d2 h.

To obtain our bifunctional amine-based **KSU-1** MOF catalysts, we incubated **KSU-1** in a 0.2M solution of the respective isocyanate in acetonitrile at 80 °C; **KSU-1** reacted with isopropyl, *tert*-butyl, *n*-hexyl and tetradecyl isocyanate to generate **KSU-1**_{Pr} and **KSU-1**_{Bu}, **KSU-1**_{Hex}, and **KSU-1**_{C14} respectively. Successful post synthetic reaction was observed by proton nuclear magnetic resonance (¹H-NMR) spectroscopy of the

MOF product digested in D₂SO₄/d₆-DMSO (**Figure 2B**). We observed that the reactions with isopropyl isocyanate and *tert*-butyl isocyanate required 3 and 4 hours respectively to achieve complete conversion at the hydroxyl without any amine reaction. With *n*-hexyl isocyanate and tetradecyl isocyanate, reaction at the amine was observed after just one hour, before complete conversion at the hydroxyl. To prevent excessive reaction at the amine, both reactions were stopped at 2 hours.

Aside from ¹H-NMR, the independent functionalization of **KSU-1** with isocyanates was also confirmed by conducting electrospray ionization mass spectrometry (ESI-MS) on samples of the MOF products digested by 1,4-diazabicyclo[2.2.2]octane (DABCO) (Figures S1-S2). For **KSU-1**_{Pr} and **KSU-1**_{tBu}, the mass spectra in negative mode had [M-H⁺] peaks corresponding to deprotonated BDC-NH₂, while in the positive mode, the [M+H⁺] peaks indicated the presence of the protonated DPG dicarbamates, along with their various fragmentation products. The mass spectra for **KSU-1**_{nHex} and **KSU-1**_{C14}, show evidence of urea products in negative mode, and protonated DPG carbamates along with their fragmentation products in positive mode (Figures S2-S4). Powder X-ray diffraction (PXRD) confirmed that crystallinity was preserved even after complete functionalization of DPG (Figure S5).

To test the catalytic behavior of our amine-based hydrophobic MOF catalysts, we chose the Knoevenagel reaction between benzaldehyde and malononitrile to form benzylidenemalononitrile (BMN, **Figure 3A**). In the initial trial, 12 mol % of the MOF catalyst was added to a vial containing benzaldehyde, malononitrile, toluene solvent, and dodecane internal standard, and the reaction was shaken at 50°C. Aliquots were collected at 30 minutes and diluted in CDCl₃ and conversions were determined by analyzing the ¹H-NMRs of the samples (**Figure 3B**).

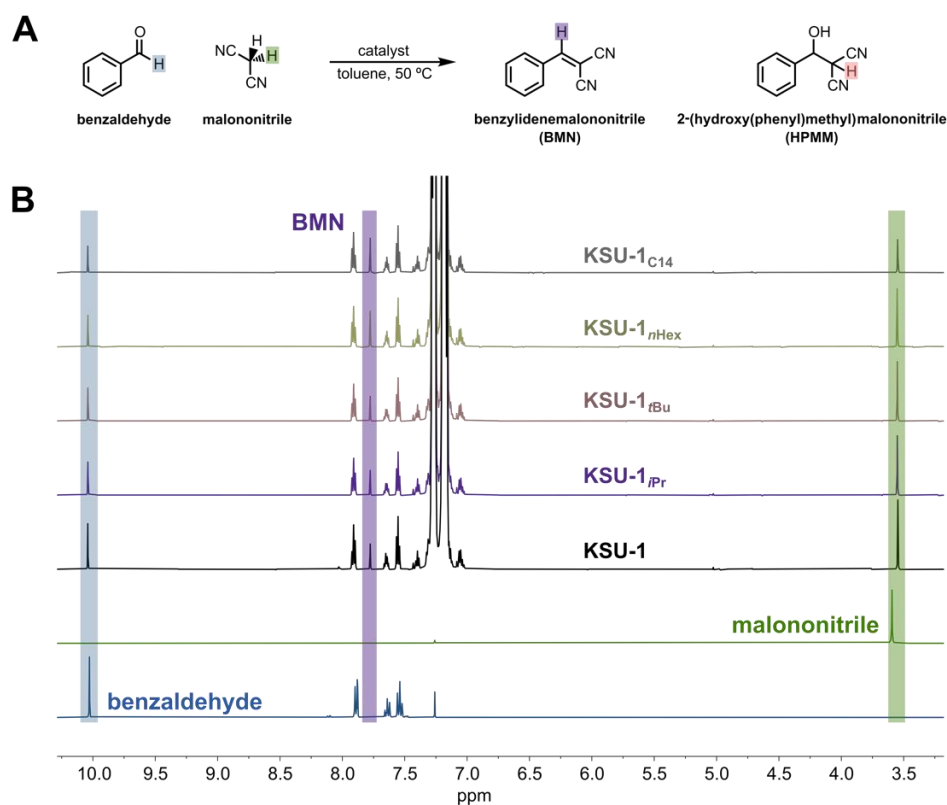


Figure 3: (A) Schematic representation of the reaction between benzaldehyde and malononitrile to form benzylidenemalononitrile (BMN). (B) Representative $^1\text{H-NMR}$ for the reaction of benzaldehyde and malononitrile in toluene with dodecane as internal standard, analyzed after 30 minutes.

The results showed a general increase in catalysis efficiency as we increased the hydrophobicity of the MOF pores. However, the observed differences in conversion between the hydrophobized catalysts was marginal, with a variation of $\sim 8\%$ (**Table 2A**). We were concerned that dodecane, our aliphatic internal standard, was negatively affecting our results by decreasing the difference in hydrophobicity between the MOF pores and the extra-MOF solution. Comparing the conversions we obtained using the dodecane calibration curve with those determined by directly comparing the integrations of the benzaldehyde and BMN protons in the $^1\text{H-NMR}$ spectra, we found little difference (**Table S1**), thus, we decided to discontinue the addition of internal standard to our catalysis reactions.

Table 2: Comparison of Knoevenagel catalysis results under different conditions.^a

Entry	Catalyst	% Conversion			
		A. Toluene+dodecane ^b	B. Toluene ^c	C. Toluene ^d	D. Neat ^e
1	no catalyst	0 (0)	0 (0)	0 (0)	3.5 (1)
2	KSU-1	36 (2)	8 (1)	3 (0)	43 (2)
3	KSU-1 _{Pr}	48 (1)	19 (2)	3 (0.5)	56 (3)
4	KSU-1 _{tBu}	51 (1)	23 (4)	2.5 (0.5)	65 (5)
5	KSU-1 _{nHex}	51 (1)	15 (3)	5 (1)	67 (5)
6	KSU-1 _{C14}	56 (3)	16 (5)	8 (0)	77 (5)

^a0.0625 mmol benzaldehyde, 0.068 mmol malononitrile, 50 °C; ^b12 mol% catalyst, 0.083 mmol dodecane, 250 μL toluene; ^c12 mol% catalyst, 250 μL toluene; ^d1.5 mol% catalyst, 250 μL toluene; ^e1.5 mol% catalyst.

Performing the reaction without dodecane revealed significantly lower conversions, and our anticipated trend in catalyst efficiency, i.e. increasing conversions with the increasing hydrophobicity of the carbamate substituents, was not consistently followed (**Table 2B**). While conversions increased going from no substitution, to isopropyl, then *tert*-butyl, subsequent increases in hydrophobicity with *n*-hexyl and tetradecyl resulted in decreased conversions at 30 minutes; a trend that can be more clearly perceived in **Figure 4A**. This result led us to speculate that the use of hydrophobic toluene as our solvent likely also decreased the difference in relative hydrophobicity between the interior and exterior of the MOF pores. Thus, we thought to run the Knoevenagel reaction under neat conditions. However, because solvents improve the solubility of the reactants and products, making it easier for the reagents to reach the active sites, we were concerned that performing the reaction neat would be detrimental: malononitrile is a solid *and* the rapid formation of solid product BMN often results in a thick sludge that hinders the flow of the reaction solution.

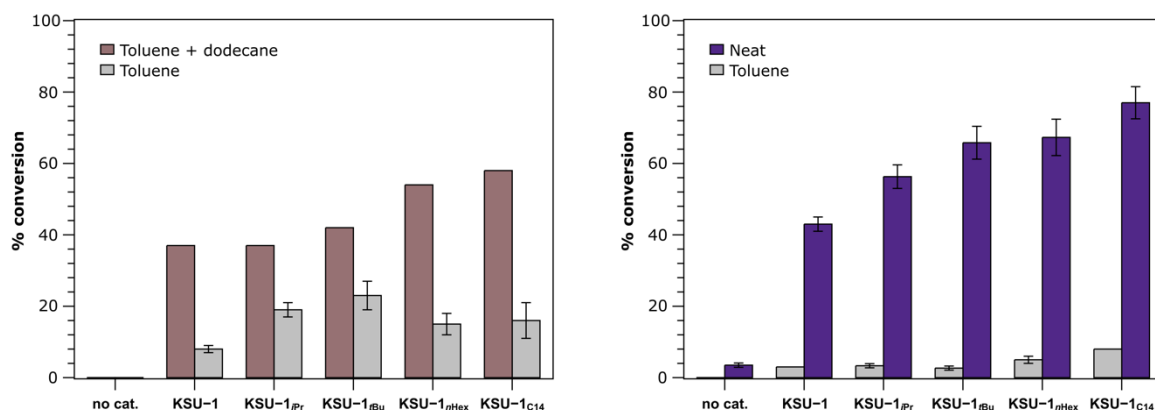


Figure 4: Graphical representation of Knoevenagel catalysis results. A: Comparison of the reaction in toluene with and without internal standard using 12 mol % catalyst. B: Catalysis performed under neat conditions and in toluene using 1.5 mol % catalyst.

To ensure that the MOFs were completely submerged in the reaction mixture, we reduced the catalyst amount to 1.5 mol %. Interestingly, the reaction conversions were higher than those in toluene with 12 mol % catalyst, and significantly so (ca. 10-fold) with a more appropriate comparison at the same catalyst loading of 1.5 mol% (**Table 2C-D**). Further to our delight, **KSU-1_{C14}** was the most active catalyst achieving 77 % conversion vs 43 % for **KSU-1** after 30 mins. In addition, a remarkably clear and gradual increase in the rate of reaction was observed from **KSU-1**<**KSU-1_{iPr}**<**KSU-1_{tBu}**<**KSU-1_{nHex}**<**KSU-1_{C14}** (**Figure 4B**) even though roughly 10% of the –NH₂ groups in both **KSU-1_{nHex}** and **KSU-1_{C14}** had been converted to the less catalytically active alkyl ureas.[46] We should also point out that, although the introduction of large alkyl substituents in a MOF is associated with a reduction in pore accessibility, the lower percentage of alkyl grafting for both **KSU-1_{nHex}** and **KSU-1_{C14}** results in similar solvent accessible volumes for all the modified MOFs, as shown by thermogravimetric analysis (TGA; Figure S6). Thus, our results indicate that catalytic efficiency improves with the increasing hydrophobicity of the alkyl chains, which is a result of the increase in surface area of the alkyl groups.[47]

Finally, we emphasize that our study was not geared toward obtaining particular conversions with our catalysts, but rather at investigating the effect that systematic pore environment modulation has on catalyst reactivity; specifically, how hydrophobization affects a condensation process like the Knoevenagel reaction. As such, it was also interesting to observe differences in the relative amount of reaction intermediate depending on the hydrophobicity of the pores. Under solvent-free conditions, we observed the formation of 2-(hydroxy(phenyl)methyl)malononitrile (HPMM, **Figure 5**), an intermediate which is subsequently dehydrated to yield the main product (BMN) as the reaction progresses.[48] Looking at the ratio of final product to intermediate (BMN:HPMM), we saw that relatively more of the hydroxyl intermediate was observed with the unfunctionalized KSU-1 catalyst (**Table 3, Entry 2**) when compared to the hydrophobicized catalysts, with the amount of HPMM decreasing with increasing aliphatic chain surface area. This trend suggests that the hydrophobic surfaces may destabilize hydrophilic intermediates, promoting faster conversion of HPMM to BMN, similar to the ground state destabilization of polar substrates observed in enzymes with hydrophobic pockets.[49,50]

Table 3: Ratio of BMN:HPMM product.^a

Entry	Catalyst	BMN:HPMM
1	no catalyst	0.3:1
2	KSU-1	4.3:1
3	KSU-1_{Pr}	10:1
4	KSU-1_{tBu}	15:1
5	KSU-1_{nHex}	17:1
6	KSU-1_{C14}	23:1

^aNeat, 50 °C, 1.5 mol% catalyst.

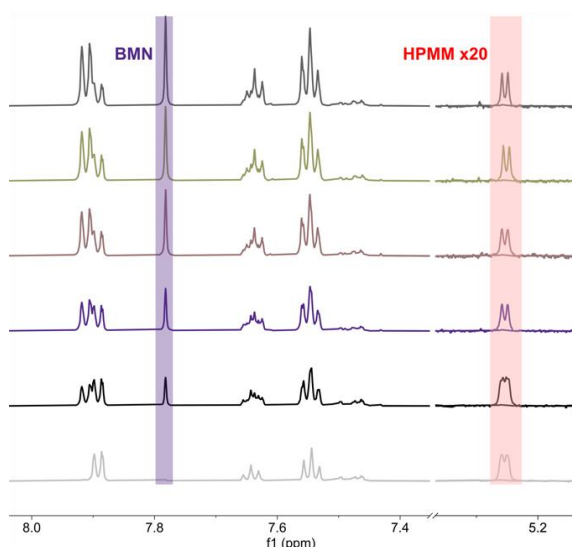


Figure 5: Comparison of BMN and HPMM protons in $^1\text{H-NMR}$.

Conclusion

By employing a covalent post synthesis modification strategy that selectively introduces hydrophobic functionality into MOFs, we confined catalytically active amines within MOF pores of systematically increasing hydrophobicity. Our results reveal a clear correlation between increased pore hydrophobicity and enhanced catalytic activity. Additionally, increasing hydrophobicity resulted in congruent changes in the distribution of intermediate versus product during the reaction. Both these behaviors, increased efficiency and different intermediate:product distributions, call to mind the effect of hydrophobic pockets in enzyme catalysis, and they offer a view to the possibilities that can be achieved in enzyme-inspired catalysis via the rational functionalization of MOF pores.

Supporting Information

Supporting information available.

Supporting Information File 1:

File Name: Matseketsa et al-SI

File Format: PDF

Title: Systematic Pore Hydrophobization to Enhance the Efficiency of an Amine-Based MOF Catalyst – Supporting Information

Funding

We thank the National Science Foundation for support of this work. Specifically, we acknowledge support to our lab (Grant CHE-2240021), as well as an NSF-MRI grant to Kansas State University for the acquisition of the NMR spectrometer (Grant CHE-1826982) used in this study. We thank the Ping Li Lab for high-resolution mass spectrometry, and the NIH for the grant (R01GM117259-01S1) which partially funded the purchase of the instrument.

References

- (1) Pravda, L.; Berka, K.; Svobodová Vařeková, R.; Sehnal, D.; Banáš, P.; Laskowski, R. A.; Koča, J.; Otyepka, M. *BMC Bioinformatics* **2014**, *15*, 379. doi:10.1186/s12859-014-0379-x
- (2) Marques, S. M.; Brezovsky, J.; Damborsky, and J. Role of Tunnels and Gates in Enzymatic Catalysis. In *Understanding Enzymes*; Jenny Stanford Publishing, 2016
- (3) Zhang, Z.; Cai, Y.; Zheng, N.; Deng, Y.; Gao, L.; Wang, Q.; Xia, X. *Biotechnol. Adv.* **2024**, *72*, 108346. doi:10.1016/j.biotechadv.2024.108346
- (4) Knowles, J. R. *Nature* **1991**, *350*, 121–124. doi:10.1038/350121a0
- (5) Zhang, X.; Houk, K. N. *Acc. Chem. Res.* **2005**, *38*, 379–385. doi:10.1021/ar040257s
- (6) Klinman, J. P.; Offenbacher, A. R.; Hu, S. *J. Am. Chem. Soc.* **2017**, *139*, 18409–18427. doi:10.1021/jacs.7b08418
- (7) Cragg, P. J. Supramolecular Enzyme Mimics. In *Supramolecular Chemistry: From Biological Inspiration to Biomedical Applications*; Cragg, P. J., Ed.; Springer Netherlands: Dordrecht, 2010; pp 113–151. doi:10.1007/978-90-481-2582-1_4
- (8) Raynal, M.; Ballester, P.; Vidal-Ferran, A.; Leeuwen, P. W. N. M. van. *Chem. Soc. Rev.* **2014**, *43*, 1734–1787. doi:10.1039/C3CS60037H
- (9) Kuah, E.; Toh, S.; Yee, J.; Ma, Q.; Gao, Z. *Chem. Eur. J.* **2016**, *22*, 8404–8430. doi:10.1002/chem.201504394
- (10) Wulff, G. *Chem. Rev.* **2002**, *102*, 1–28. doi:10.1021/cr980039a

- (11) Li, S.; Zhu, M.; Whitcombe, M. J.; Piletsky, S. A.; Turner, A. P. F. *Molecularly Imprinted Polymers for Enzyme-like Catalysis: Principle, Design, and Applications*. In *Molecularly Imprinted Catalysts*; Elsevier: Amsterdam, 2016; pp 1–17. doi:10.1016/B978-0-12-801301-4.00001-3
- (12) Bahrami, F.; Zhao, Y. *Org. Lett.* **2024**, *26*, 73–77. doi:10.1021/acs.orglett.3c03666
- (13) Bhaskaran, A.; Aitken, H. M.; Xiao, Z.; Blyth, M.; Nothling, M. D.; Kamdar, S.; O'Mara, M. L.; Connal, L. A. *Polymer* **2021**, *225*, 123735. doi:10.1016/j.polymer.2021.123735
- (14) Margelefsky, E. L.; Zeidan, R. K.; Davis, M. E. *Chem. Soc. Rev.* **2008**, *37*, 1118–1126. doi:10.1039/B710334B
- (15) Shylesh, S.; Wagner, A.; Seifert, A.; Ernst, S.; Thiel, W. R. *Chem. Eur. J.* **2009**, *15*, 7052–7062. doi:10.1002/chem.200900851
- (16) Chandra, P.; Jonas, A. M.; Fernandes, A. E. *J. Am. Chem. Soc.* **2018**, *140*, 5179–5184. doi:10.1021/jacs.8b00872
- (17) Fernandes, A. E.; Jonas, A. M. *Catal. Today* **2019**, *334*, 173–186. doi:10.1016/j.cattod.2018.11.040
- (18) Zhang, M.; Gu, Z.-Y.; Bosch, M.; Perry, Z.; Zhou, H.-C. *Coord. Chem. Rev.* **2015**, *293–294*, 327–356. doi:10.1016/j.ccr.2014.05.031
- (19) Fracaroli, A. M.; Siman, P.; Nagib, D. A.; Suzuki, M.; Furukawa, H.; Toste, F. D.; Yaghi, O. M. *J. Am. Chem. Soc.* **2016**, *138*, 8352–8355. doi:10.1021/jacs.6b04204
- (20) Zhang, Y.; Gui, B.; Chen, R.; Hu, G.; Meng, Y.; Yuan, D.; Zeller, M.; Wang, C. *Inorg. Chem.* **2018**, *57*, 2288–2295. doi:10.1021/acs.inorgchem.7b03123
- (21) Liu, J.; Chen, L.; Cui, H.; Zhang, J.; Zhang, L.; Su, C.-Y. *Chem. Soc. Rev.* **2014**, *43*, 6011–6061. doi:10.1039/C4CS00094C
- (22) Alhumaimess, M. S. *J. Saudi Chem. Soc.* **2020**, *24*, 461–473. doi:10.1016/j.jscs.2020.04.002
- (23) Garibay, S. J.; Wang, Z.; Cohen, S. M. *Inorg. Chem.* **2010**, *49*, 8086–8091. doi:10.1021/ic1011549
- (24) Liu, L.; Zhou, T.-Y.; Telfer, S. G. *J. Am. Chem. Soc.* **2017**, *139*, 13936–13943. doi:10.1021/jacs.7b07921
- (25) Zhou, T.-Y.; Auer, B.; Lee, S. J.; Telfer, S. G. *J. Am. Chem. Soc.* **2019**, *141*, 1577–1582. doi:10.1021/jacs.8b11221
- (26) Cohen, S. M. *Chem. Rev.* **2012**, *112*, 970–1000. doi:10.1021/cr200179u
- (27) Kalaj, M.; Cohen, S. M. *ACS Cent. Sci.* **2020**, *6*, 1046–1057. doi:10.1021/acscentsci.0c00690
- (28) Chui, S. S.-Y.; Lo, S. M.-F.; Charmant, J. P. H.; Orpen, A. G.; Williams, I. D. *Science* **1999**, *283*, 1148–1150. doi:10.1126/science.283.5405.1148
- (29) Rosi, N. L.; Kim, J.; Eddaoudi, M.; Chen, B.; O'Keeffe, M.; Yaghi, O. M. *J. Am. Chem. Soc.* **2005**, *127*, 1504–1518. doi:10.1021/ja045123o
- (30) Gadzikwa, T.; Matseketsa, P. *Dalton Trans.* **2024**. doi:10.1039/D4DT00514G
- (31) Canivet, J.; Aguado, S.; Daniel, C.; Farrusseng, D. *ChemCatChem* **2011**, *3*, 675–678. doi:10.1002/cctc.201000386
- (32) Liu, L.; Tao, Z.-P.; Chi, H.-R.; Wang, B.; Wang, S.-M.; Han, Z.-B. *Dalton Trans.* **2021**, *50*, 39–58. doi:10.1039/D0DT03635H
- (33) Joharian, M.; Morsali, A.; Tehrani, A. A.; Carlucci, L.; M. Proserpio, D. *Green Chem.* **2018**, *20*, 5336–5345. doi:10.1039/C8GC02367K
- (34) Breslow, R. *J Phys. Org. Chem.* **2006**, *19*, 813–822. doi:10.1002/poc.1037
- (35) Blaha-Nelson, D.; Krüger, D. M.; Szeler, K.; Ben-David, M.; Kamerlin, S. C. L. *J. Am. Chem. Soc.* **2017**, *139*, 1155–1167. doi:10.1021/jacs.6b10801

- (36) Appaturi, J. N.; Ratti, R.; Phoon, B. L.; Batagarawa, S. M.; Din, I. U.; Selvaraj, M.; Ramalingam, R. J. *Dalton Trans.* **2021**, *50*, 4445–4469. doi:10.1039/D1DT00456E
- (37) Rupainwar, R.; Pandey, J.; Smrirti; Ruchi. *Orient. J. Chem.* **2019**, *35*, 423–429
- (38) Freeman, F. *Chem. Rev.* **1980**, *80*, 329–350. doi:10.1021/cr60326a004
- (39) Prout, F. S. *J. Org. Chem.* **1953**, *18*, 928–933. doi:10.1021/jo50014a005
- (40) Saghian, M.; Dehghanpour, S.; bayatani, Z. *Sci Rep* **2023**, *13*, 15563. doi:10.1038/s41598-023-42832-5
- (41) Zarei, N.; Yarie, M.; Torabi, M.; Zolfigol, M. A. *RSC Adv.* **2024**, *14*, 1094–1105. doi:10.1039/D3RA08354C
- (42) Calvino-Casilda, V.; Martín-Aranda, R. M.; López-Peinado, A. J.; Sobczak, I.; Ziolk, M. *Catal. Today* **2009**, *142*, 278–282. doi:10.1016/j.cattod.2008.08.023
- (43) Samarakoon, K. P.; Satterfield, C. S.; McCoy, M. C.; Pivaral-Urbina, D. A.; Islamoglu, T.; Day, V. W.; Gadzikwa, T. *Inorg. Chem.* **2019**, *58*, 8906–8909. doi:10.1021/acs.inorgchem.9b00838
- (44) Matseketsa, P.; Mafukidze, D.; Pothupitiya, L.; Otuonye, U. P.; Mutlu, Y. Ç.; Averkiev, B. B.; Gadzikwa, T. *Mol. Syst. Des. Eng.* **2024**. doi:10.1039/D3ME00185G
- (45) Samarakoon, K. P.; Satterfield, C. S.; McCoy, M. C.; Pivaral-Urbina, D. A.; Islamoglu, T.; Day, V. W.; Gadzikwa, T. *Inorg. Chem.* **2019**, *58*, 8906–8909. doi:10.1021/acs.inorgchem.9b00838
- (46) van Schijndel, J.; Canalle, L. A.; Molendijk, D.; Meuldijk, J. *GCLR* **2017**, *10*, 404–411. doi:10.1080/17518253.2017.1391881
- (47) Lee, A.; Mirica, K. A.; Whitesides, G. M. *J. Phys. Chem. B* **2011**, *115*, 1199–1210. doi:10.1021/jp107765h
- (48) Antonangelo, A. R.; Hawkins, N.; Tocci, E.; Muzzi, C.; Fuoco, A.; Carta, M. *J. Am. Chem. Soc.* **2022**, *144*, 15581–15594. doi:10.1021/jacs.2c04739
- (49) Biler, M.; Crean, R. M.; Schweiger, A. K.; Kourist, R.; Kamerlin, S. C. L. *J. Am. Chem. Soc.* **2020**, *142*, 20216–20231. doi:10.1021/jacs.0c10701
- (50) Chen, D.; Li, Y.; Li, X.; Hong, X.; Fan, X.; Savidge, T. *Chem. Sci.* **2022**, *13*, 8193–8202. doi:10.1039/D2SC01994A